DESIGN AND DEVELOPMENT OF 3D POINT CLOUD SCANNER SYSTEM (3D-PCSS) WITH A WEB-BASED INTERFACE FOR FLOUR PRODUCT STORAGE VOLUME MEASUREMENT

A THESIS

Presented to the Faculty of
Department of Computer Applications
College of Computer Studies
Mindanao State University – Iligan Institute of Technology

In Partial Fulfillment
of the Requirements for the Degree
MASTER OF SCIENCE IN COMPUTER APPLICATIONS

JAAFAR J. OMAR

ENGR. CARL JOHN O. SALAAN, Ph.D.
Adviser

March 2023

CONTENTS

LIST OF FIGURES

LIST OF TABLES

CHAPTER I

INTRODUCTION

1.1 Background of the Study

Agricultural raw materials, such as rice, wheat, and corn, which mostly include solid, liquid or powered, provide significant amounts of carbohydrates for use in industry and human nutrition . Certain grains require little processing and can be eaten right away after harvest, while others must be prepared through a number of primary and secondary milling steps. As farmers learned to produced more resulting of various agricultural innovation, this raw materials must preserve the quality for future consumption (Bucklin et al., 2019). It is expected an increase in raw materials annually does necessitate an efficient post-harvest processes such as raw product storing method incorporating modern technologies (Kumar and Kalita, 2017; Yegorova et al., 2021; Munarso et al., 2022).

Various tools and methods have been developed to measure stored raw materials volume inside an industrial storage silos or bins, employing sen-

sors like contact level indicators (e.g., tilt switches, pressure diaphragms, rotary paddles) and non-contact indicators (e.g., stereovision, radar, ultrasound, lasers). Contact sensors offer cost-effective, dust-resistant point measurements but lack surface detail. Non-contact sensors can map grain surfaces accurately but require permanent mounting, are relatively expensive, and are susceptible to dust interference. However, conventional volumetric measurement method using weighted fiberglass tape is still being used providing only a single data point which leads to inaccuracy and error-prone volume measurement (Turner et al., 2016, 2017).

Point cloud data consists of a set of points representing an object in either a two or three-dimensional structure. This data typically comprises X, Y, and Z coordinates, but modern point clouds may also include additional information such as intensity, RGB values, and more (Wang and Kim, 2019; Stojanovic, 2023).

Light Detection and Ranging (LiDAR) is one of the many devices that can gather 3D points that often refer as point clouds. Unfortunately, commercial 3D LiDAR systems tend to be expensive in comparison to their 2D-based LiDAR. This cost disparity can lead to limitations in accessibility for certain applications or industries, hindering widespread adoption and innovation in fields where 3D spatial data is crucial. Low-cost two axes-based LiDAR can mimic the collection of 3D point cloud by adding an additional axes using tilting device (Clar and Salaan, 2022). However, it comes with

a notable drawback: it lacks several capabilities present in high-end 3D LiDAR systems, including multi-echo functionality, long-range detection, high angular resolution, among others.

Recent innovations in various industries have made the production less manual but producing more by using automation and wireless technologies that helped to produce better and accurate measurement compared to traditional methods. These approaches include various sensing technologies, automated measurements, machine to machine (M2M) communications, and monitoring systems. The interconnected sensors and actuators allow to remotely collect data, store, and process the data to provide better insight in the industry and also for the economic growth, specify the characteristics of a paperless factory, it is a development of a smart factory in which all data that is turned into information is stored, transferred, and displayed entirely remotely and digitally. As the level of digitization of a smart factory, it is not a revolution but rather an evolution (Bulut et al., 2020).

1.2 Statement of the Problem

While some food manufacturing industries still rely on manual and labor-intensive storage measurement procedures, there is a growing need to adopt advanced technologies with remote capabilities. This shift aims to eliminate the need for frequent physical processes that may endanger employees. Additionally, monitoring the volume of raw product storage, par-

ticularly in industries dealing with essential commodities like flour, holds paramount importance for various reasons. Ensuring accurate and timely monitoring of storage bins prevents detrimental scenarios such as underproduction or overstocking. In the case of underproduction, inadequate monitoring leading to stockouts can disrupt the production process, resulting in delayed deliveries and potential loss of sales. Conversely, overstocking can lead to unnecessary inventory costs, space constraints, and increased risk of product spoilage or infestation. Specifically, in the context of flour storage, overstocking can attract flour beetles, leading to infestation and contamination of the stored flour when left unsold. Thus, precise volume monitoring is crucial to maintaining optimal inventory levels, facilitating efficient production planning, and mitigating the risk of financial losses and product quality issues for food manufacturing industries.

This study presents the development of a volumetric measurement system for raw materials storage bin. The system is designed to be controlled and scanned remotely using a web-based interface, alleviating the manual process of volume measurement. Additionally, this study investigates the behavior of the system when dust clouds are present during filling due to fine texture of some raw materials such as flour.

1.3 Objectives of the Study

The general objective of this study was to develop a system that can remotely measure the volume of the product inside of a flour storage bin using point cloud data and web-based Application. The following specific goals were completed:

1. Designed and developed a 3D point cloud scanner system (3D-PCSS);

2. Developed a web-based application for remote access to 3D-PCSS system and visualization for point cloud and volume measurement;

3. Tested and evaluated the performance of the system.

1.4 Originality of the Study

The originality of this study lies in the development of a system capable of remotely estimating and monitoring the volume and capacity of storage materials. This study introduces two distinct components: the point cloud acquisition system and the web application system designed for remote monitoring purposes. Furthermore, the study explores the system's behavior in the presence of dust, providing insights for further enhancement and modification.

1.5   Scope and Limitations

The scope of this study is to develop a volume estimation system through remote point cloud acquisition and a web application. It is important to note that the system testing was not conducted directly in a commercial manufacturing industry or an actual industrial storage bin. Instead, testing took place in an open area using a mock-up storage bin designed to replicate the size and shape of a typical industrial storage facility. Additionally, the study exclusively focuses on utilizing flour as the primary raw material for testing purposes.

1.6   Significance of the Study

Accurate and efficient post-harvest processes are vital in the food industry to ensure effective inventory management and maintain an adequate supply of materials. Automation with remote sensing devices is a modern technology that can be integrated into a variety of industries, eliminating labor-intensive tasks that may expose employees to dangerous scenarios. The development of the 3D point cloud scanner system (3D-PCSS) addresses the need for precise volume measurement of stored flour within silo storage bins. By employing point cloud data and a web-based application, the system offers remote accessibility and visualization capabilities, allowing for convenient monitoring and management of storage facilities. This

technological advancement, with potential integration into industrial settings, not only enhances efficiency in inventory management but also minimizes the risks associated with manual measurement procedures. Furthermore, the testing and evaluation of the system provide valuable insights into its performance and potential for further refinement, paving the way for future advancements in automated storage volume measurement systems.

1.7 Conceptual Framework

INPUTS

Existing Storage Volume Measurement Methods

3D Point Cloud Acquisition Methods and Devices

User Interface for Remote Monitoring

PROCESS

Conceptualization of 3D Point Cloud Scanner and User Interface

Conceptualization of Firmware Development

Integration of the Overall System

OUTPUT

3D Point Cloud Scanner System with A Web-based Application for Storage Volumetric Measurement

Figure 1.1. General Conceptual Flow

Figure 1.7 outlines the conceptualization of the study. As shown in the figure, The conceptualization of the study are derived from the examination of prior studies and established methodologies. The study examined existing storage volume measurement methods, 3D point cloud acquisition methods and devices, and different user interface for remote monitoring. The output of this paper is the design and development 3D point cloud scanner system with a web-based application for Storage volumetric measurement. The general and specific objectives are presented in the previous section (see section 1.3).

1.8 Theoretical Framework

This section introduces the fundamental theories that guides the underlying principles, methodologies and technologies involved in the study.

1.8.1 Calculating Storage Materials Volume using Depth Measurement

The volume of stored grain is typically calculated using the depth measurement. Once the equivalent level height of the grain is determined based on the depth measurement and surface profile assessment, this height is multiplied by the conversion factor to obtain the volume of the stored grain. This calculation accounts for the headspace between the eave and the grain surface. The underlying calculation with a single and non complex geometric shape can be presented as follows:

$$V = A \times h \tag{1.1}$$

Where:

$$V : \text{Volume of the storage container}$$

$$A : \text{Area of the base of the container}$$

$$h : \text{Height or depth of the container}$$

1.8.2 3D Polar Coordinate to Cartesian Coordinate

Converting polar coordinates to cartesian coordinates in three dimensions involves considering the radial distance (ρ), the polar angle (θ), and the azimuthal angle (ϕ). Given a point in spherical coordinates (ρ, θ, ϕ), the corresponding Cartesian coordinates (x, y, z) can be calculated as follows:

$$x = \rho \times \sin(\theta) \times \cos(\phi) \tag{1.2}$$

$$y = \rho \times \sin(\theta) \times \sin(\phi) \tag{1.3}$$

$$z = \rho \times \cos(\theta) \tag{1.4}$$

Where: x, y, and z represent the Cartesian coordinates of the point. ρ is the radial distance from the origin to the point. θ is the polar angle

measured from the positive z-axis to the point. ϕ is the azimuthal angle measured from the positive x-axis to the projection of the point onto the xy-plane.

1.8.3 Point Cloud Data

A set of points in three dimensions that represent an object's or scene's surface is called a point cloud. Point clouds can be generated through a variety of methods, including photogrammetry, LiDAR, and 3D scanning. Processing and evaluation of these point clouds for a variety of applications is an increasing area of point cloud processing.

1.8.4 Computational Geometry using Convex Hull

The study of the development and evaluation of algorithms for geometric problems in low dimensions—usually two or three—is known as computational geometry. As the smallest convex polygon containing a given set of points, the Convex Hull is a fundamental concept in computational geometry. The convex hull represents the smallest convex set enclosing a given set of points in a Euclidean space as figure 1.2 illustrated. It adheres to principles of convexity, ensuring that the shape remains convex, and minimality, guaranteeing it encompasses the points with minimal expansion.

The Gift Wrapping algorithm, which has a time complexity of O(nh), where n is the number of points and h is the number of points on the hull, is

one straightforward method for calculating the Convex Hull (Barber et al., 1996; Chan, 1996).

The equation 1.5 defines the convex hull of a set of points P_j in N-dimensional space. The variable C represents a point in the convex hull, λ_j are non-negative weights, and A_j are some constraints. The summation iterates over all points from $j = 1$ to N.

$$C = \left\{ \sum_{j=1}^{N} \lambda_j P_j : \lambda_j \geq 0 \text{ for all } j \text{ and } \sum_{j=1}^{N} \lambda_j = 1 \right\} \tag{1.5}$$
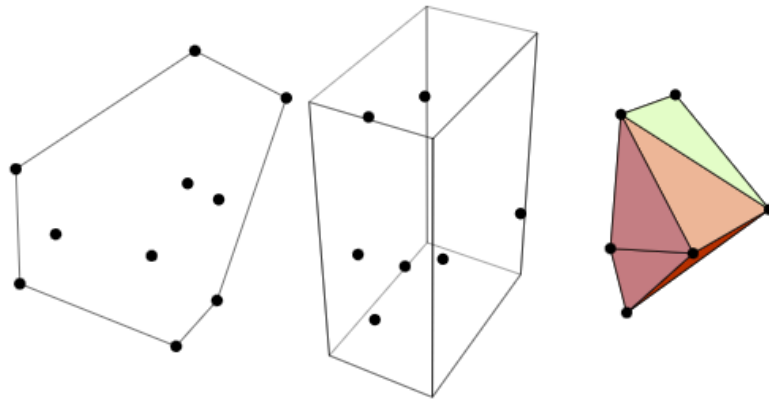

Figure 1.2. Convex Hull of Set of Points

TODO: Add Polygon Mesh

1.8.5 ROS Nodes, Topics, and Subscribe-Publish Relationship

A framework for building complicated robotic systems that is adaptable is called Robot Operating System (ROS). It makes it possible for nodes,

software components that carry out particular functions, to communicate with one another. Topics, also referred to as buses, are the methods by which nodes exchange messages with one another. A key component of ROS is the publish-subscribe connection, in which nodes can publish or subscribe to topics.

Nodes in ROS have the ability to simultaneously subscribe to an indefinite number of topics and share data to an indefinite number of topics. One of the main methods of data communication between nodes, and consequently between other components of the system, is through topics (St-Onge and Herath, 2022). A node must first advertise a topic before publishing content, or messages, into it in order to exchange information. The first part is completed in the node's initialization code, and the second is completed each time new data has to be shared, usually at a predetermined frequency inside the main loop of the code. Conversely, the node or nodes that need the content of a topic will subscribe to it. The subscriber will associate a callback function triggered for each new incoming message (St-Onge and Herath, 2022).

1.9   Definition of Terms

1. **LiDAR** —stands for Light Detection and Ranging, can also be describe as Light Imaging, Detection, and Ranging. It is a method for determining ranges by targeting an object or a surface with a laser and measur-

ing the time-of-flight to determine the distance.

2. **Bin** —is a large container used to store materials, such as grain, coal, sand, or other bulk goods. They are typically made of metal, plastic, or wood and come in various sizes, shapes, and designs.

3. **ROS** —Robot Operating System is a set of open-source libraries and tools designed to help developers build robot applications. It provides a common framework for creating, managing and sharing code, data, and other resources related to robotic systems.

4. **Point Cloud** —is a set of data points in a three-dimensional space, typically representing the surface of an object. Each point in the cloud is defined by its three-dimensional coordinates (x, y, and z) and may also include additional information such as color, intensity, or normal vector.

5. **Convex Hull** —is the minimum convex polygon from the set of points that encompasses all of the points in the set.

CHAPTER II

REVIEW OF RELATED LITERATURE

Enhancing post-harvest processing and storage technology is essential meeting increasing global demand and minimizing waste. Improved technology ensures efficient supply chains and reduces losses due to spoilage, damage, or inefficient methods. Moreover, advanced monitoring and management techniques not only enhance production but also contribute to safety standards (Kumar and Kalita, 2017; Munarso et al., 2022).

In this chapter, various relate topic were reviewed and discussed. Different methods, technologies and implementation were also introduced and examined.

2.1 Overview of Existing Methods, Techniques and Technologies Used for Volume Measurement

According to Turner et al. (2016), the determination of grain volume in a bin depends on variables like bin diameter and corresponding level height of grain. Different surface condition assessment, however, is subjec-

tive and subject to a number of variables, such as operator experience, visibility, lighting, and ambient circumstances. Various strategies can be used to improve volume estimate; standard angles of repose for various grain types are provided in the literature.

Traditional level measurements are already used and studied in different industries such as weight and cable methods, ultrasonic, Guided Ware Radar (GWR), and Thru-air Radar (TAR) which has their own advantage and disadvantages. Ultrasonic and laser technologies are excellent in providing accurate and detailed measurement of level. However, these technologies are problematic when in terms of dusty environment (Duysak and Yigit, 2020). Additionally, Various tools and methods have been developed to measure stored raw materials volume inside an industrial storage silos or bins, employing sensors like contact level indicators (e.g., tilt switches, pressure diaphragms, rotary paddles) and non-contact indicators (e.g., stereovision, radar, ultrasound, lasers). Contact sensors offer cost-effective, dust-resistant point measurements but lack surface detail. Non-contact sensors can map grain surfaces accurately but require permanent mounting, are relatively expensive, and are susceptible to dust interference. However, conventional volumetric measurement method using weighted fiberglass tape is still being used providing only a single data point which leads to inaccuracy and error-prone volume measurement due to uneven materials surface topology (Turner et al., 2016, 2017).

New methods and technologies have been trying to incorporate in industrial settings to enhance the measurement methods such as using Microwaves Radar (Vogt and Gerding, 2017), Horn Antennas-based (Duysak and Yigit, 2020; Yigit et al., 2015), Load Cell, Ultrasonic, Laser-based (Guevara et al., 2020), and Temperature-based sensor (Rhee et al., 2021).

2.2   Point Cloud Acquisition Devices

The recent advancements in spatial acquisition technologies such as 3D laser scanning, photogrammetry, videogrammetry, RGB-D camera, and stereo camera have resulted in the formation of point clouds that may contain millions, billions, or trillions of points (Jaboyedoff et al., 2012). Various 3-dimensional scanning technology produces data that are formatted as point cloud, typically these point cloud data acquired using laser or image scanner. These gathered data can be managed to ease the measurement and visualization of an object or environment (Chua et al., 2017). Point cloud data are processed to generate desired output on the specific application. Over the past 20 years, the advent of high-quality 3D point cloud acquisition changes the perspective of robotics. Moreover, 3D scanning through various technologies enable the possibility of less contact for physical measurement that eliminate the traditional approach that involves time and effort. These technologies vary in size, functionality, and cost, ranging from affordable options to more complex and expensive ones (Rusu and Cousins,

2011).

2.2.1   Light Detection and Ranging (LiDAR)

LiDAR, a remote sensing technology, employs laser light to create precise 2D or 3D models of objects or environments. Apart from Time-of-Flight (ToF) and triangulation, which measures distances based on the angle and timing of laser pulses, LiDAR systems utilize other techniques such as amplitude modulation and frequency modulation. These techniques vary in how they measure distances and capture data. By integrating data from multiple laser pulses, LiDAR generates a comprehensive point cloud that accurately represents the shape and structure of the objects within the environment, Figure 2.1 shows the block diagram of a typical LiDAR system. LiDAR technology have been used in industrial settings. In the context of LiDAR scanning, individual point cloud scans are acquired and processed for a specific area. These point clouds are then merged and blended together to generate a complete point cloud of the desired area, which can be utilized for distance and measurement calculations (Jaboyedoff et al., 2012; Raj et al., 2020).
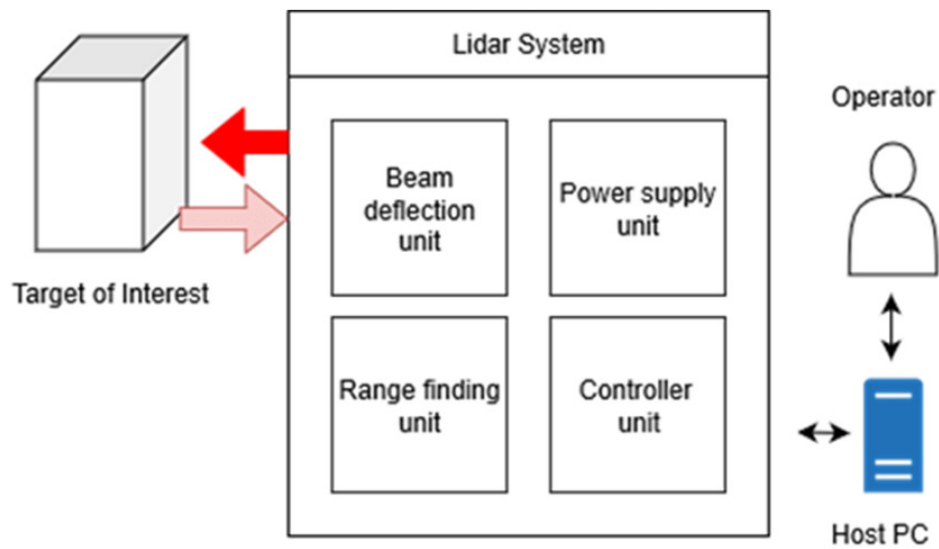
Figure 2.1. Typical LiDAR System

A 360-degree scan of a LiDAR is generally obtained as shown in figure 2.2 to produce a 2D map, a typical scan using the robot's top-mounted 2D LIDAR. The axis of the rotating LIDAR sensor is shown as a red line. The border of the surrounding obstacles is indicated in blue (Sarker et al., 2020).
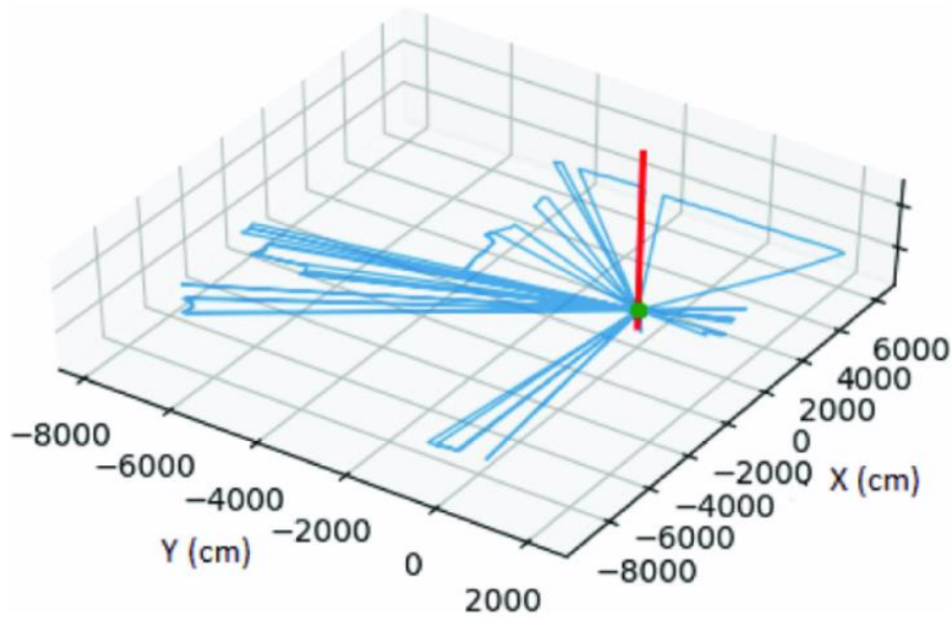
Figure 2.2. 360-degree scan of 2D LiDAR

2.2.2 Rotating 2D LiDAR Scanner into a 3D Point Cloud Scanner: Mechanisms and Techniques

A 2D LiDAR scanner, typically used for horizontal plane scanning, can be transformed into a 3D point cloud scanner with the addition of extra components and processing techniques. One common method involves incorporating a rotating mechanism, such as a pan-tilt unit (PTU), to the 2D LiDAR. As the LiDAR rotates, it collects data points at various angles, generating a series of 2D scans. These scans are then combined and processed using algorithms to reconstruct a 3D representation of the surroundings. Integrating the 2D LiDAR device with electric motors into various configurations enables the acquisition of 3D scans. Figure 2.3 illustrates four such

configurations: pitching, rolling, yawing, and top yawing scans (Raj et al., 2020).
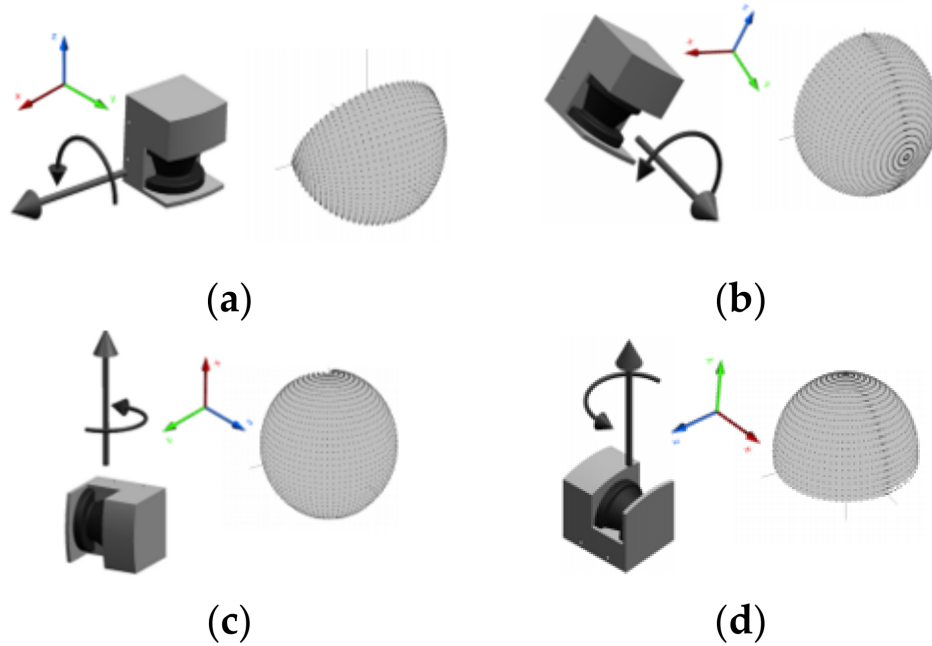
Figure 2.3. Four different configurations for rotating: (a) pitching scan, (b) rolling scan, (c) yawing scan, (d) top yawing scan

Source: (Raj et al., 2020)

Kang et al. (2018) utilized a 2D low-cost off-the-shelf LiDAR to reconstruct complex 3D model by integrating an external rotary for additional dimension. The experimental test achieved to evaluate 3D reconstruction by concluding that using a low-cost 2D LiDAR sensors can perform 3D point cloud acquisition but increase either the complexity of its hardware or software.

A stepper motor was used in the study conducted by Yuan et al. (2021) and Kang et al. (2018) to rotate a 2D LiDAR. However, in the study con-

ducted by Yuan et al. (2021), the rotating 2D LiDAR with initial motor shaft position defined using a combination of photoelectric switches and shading sheets, to create a 3D point cloud representation of the environment. The main objective of the study was to minimize the cost by utilizing stepper motor. Intensive calibration was conducted to correct the error of the system due to lack of the absolute angle position of the motor, thus, the study focus on calibrating the system by synchronizing the 2D LiDAR with the stepper motor.

In a previous study by Clar and Salaan (2022), a servo motor was employed to rotate a 2D LiDAR, with calibration performed to synchronize the LiDAR's movement. However, the system in that study relied on a laptop and microcontroller for operation. While adequate for experimental testing, this setup posed challenges for larger-scale deployment due to its size, weight, and power demands. Consequently, there arose a need for a more compact and portable solution to address these limitations.

The primary problem with calibration and synchronization between a 2D lidar and a servo arises from the lack of an absolute angle reference for the servo. Unlike encoders or sensors that provide precise angular measurements, servos typically lack absolute positioning capabilities. Although rotating 2D LiDAR can never replace commercial 3D LiDAR with several reasons, however, rotating 2D LiDAR can be partially used and installed with in terms of static and nonmoving environment (Bi et al., 2021).

TODO: ADD AUTHORS THAT USES ADDITIONAL functionality FOR 2D TO 3D

2.3 Volume Measurement Using 3D Point Cloud Data

Utilizing the latest advances in volume measurement with 3D point cloud data is an innovative method that precisely determines the volume of spaces or objects in a three-dimensional environment. This technique makes precise and thorough volumetric analysis possible by using point cloud data, which frequently consists of millions of points in 3D space. The concepts, procedures, and uses of volume measurement with 3D point cloud data will be covered in explain in this section, along with examples of its relevance in various domains (Zhi et al., 2016; Meng et al., 2023).

2.3.1 Frameworks for Point Cloud Processing, Visualization, and Mapping

Various point cloud processing and mapping frameworks are widely available to lessen the complexity of handling raw point cloud data, such as, Robotic Operating System (ROS), Point Cloud Library (PCL), Open3D, MeshLab, etc. Most of this framework can be used in many different fields such as virtual reality, construction, industry, and surveying.

The PCL has a built-in visualization library that uses Visualization ToolKit (VTK) as its foundation. VTK is a versatile platform that can render

3D point clouds and surfaces, and supports visualizing tensors, textures, and volumetric methods. The PCL Visualization library aims to merge PCL with VTK by providing a complete visualization layer for n-D point cloud structures. Its main goal is to allow for rapid prototyping and visualization of algorithm results on high-dimensional data (Rusu and Cousins, 2011).

Ocando et al. (2017) take advantage of using ROS framework to map the 3D point cloud data, as the framework allows to interlink programs that is written in different languages. The study successfully addressed the problematic tasks of Simultaneous Localization and Mapping (SLAM) and 3D Octomapping via single sensor. Clar and Salaan (2022) also utilizes ROS framework and PCL to filter, convert and measure the volume of the gathered point cloud data.

2.3.2 Techniques and Methods for Volume Estimation Using Computational Geometry

Point clouds in 3D are highly valuable as they contain crucial information on the shape, size, area, and volume of objects. Various industries, including agriculture and fisheries, have effectively utilized volume estimating methods based on point clouds (Guevara et al., 2020).

Due to a better portrayal of the region encompassed in the group of points, the Delaunay triangulation and voxelization procedures outperform in estimating the outcomes. These strategies, however, have a greater com-

putational cost because of their accuracy (Auat Cheein et al., 2015). To estimate volume, methods such as Delaunay triangulation and voxelization are used. It is important to consider both accuracy and computing costs when using these methods. Height grids are faster for computing height discrepancies, but accuracy depends on precise point acquisition (Bewley et al., 2011; Duff, 2000).

The Delaunay triangulation-based technique for volume computation, known as Delaunay triangulation-driven volume calculation (DTVC), differs from traditional approaches which computes the volume during the triangulation process rather than preserving Delaunay triangles. This method reduces both memory usage and processing time. Experimental findings demonstrate that DTVC achieves a satisfactory trade-off between precision and efficiency (Liu and Zheng, 2021).

In computer graphics, a voxel is an image that depicts a specific region that has been partitioned into a grid of cubes that are all the same size and uniformly spaced (Putman and Popescu, 2018).

The Convex Hull is another method that is popular technique for measuring volume from 3D point cloud points (see figure 2.4). The computational geometry community has extensively studied the convex hull problem, as evidenced by the works of Kim (2002), Graham and Frances Yao (1983), and Maus (1984). Qhull is a commonly used algorithm to compute the convex hull, employing the Voronoi diagram, the Delaunay triangula-

tion, furthest-site Voronoi diagram, the furthest-site Delauney triangulation, and the half-space intersection around a point. The software program allows the creation of high-dimensional objects, and the Quickhull algorithm, written in C, is used to compute the convex hull, which solves round-off errors in floating-point arithmetic. The program is capable of calculating volumes, surface areas, and convex hull approximations.
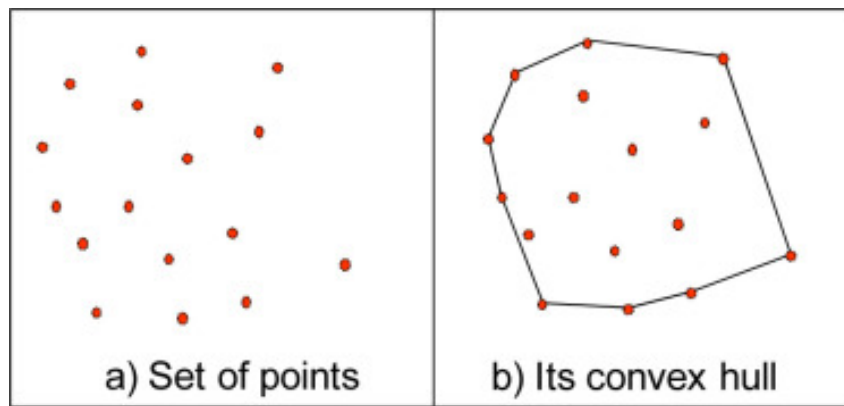
Figure 2.4. Convex Hull

Table 2.1 shows the percentage error analysis from the computed volume of different model point cloud objects in the study of Chang et al. (2017), which shows that in order to estimate the volume of a shape represented by a point cloud, the area of each slice of the shape is calculated by finding the difference between the top and bottom curves of the slice. The total volume of the shape is then calculated by integrating the areas of all the slices using an integration interval equal to the length of the point cloud.

Table 2.1. Point Cloud Volume of Different Model

Objects	True Value (mm^3)	Estimated Value (mm^3)	Error (%)
Cube	1 000 000	1 000 000	0
Cylinder	125.664	125.061	0.479
Sphere	4 188 90.2	4 178 966.87	0.234
Triangle Prism	17.321	17.399	0.45

The study conducted by Jeong et al. (2018) introduces a newly developed explicit hybrid numerical methodology for 3D volume reconstruction from unorganized point clouds, which is based on a modified Allen-Cahn equation and a 3D binary picture segmentation method. The technique has demonstrated potential in a variety of practical applications, including 3D model printing from dispersed scanned data. The computational findings show that the suggested approach for reconstructing 3D volume from point clouds is very efficient and resilient.

2.4   Robot Web Tools Application for ROS Remote Monitoring

The integration of Robot Web Tools (RWT) with ROS has garnered significant attention in recent years due to its potential to revolutionize real-time robotics applications. By leveraging web technologies and cloud computing infrastructure, developers aim to create intuitive interfaces for controlling and monitoring robots remotely. Central to the capabilities of RWT is its efficient messaging mechanism, which enables real-time interaction between web-based interfaces and ROS-enabled robots. By leveraging tech-

nologies such as roslibjs and rosbridge, RWT facilitates the seamless exchange of data, including sensor readings, point clouds, and control commands. This efficient messaging paradigm forms the backbone of RWT's ability to provide responsive and interactive interfaces for controlling and monitoring robotic systems.

Several studies have explored the capabilities of RWT in enabling real-time interaction with ROS-enabled robots. For instance, in a study by Qureshi et al. (2016), the development of a disaster management application is showcased, wherein Robot Web Tools (RWT) is utilized for seamless communication with ROS nodes. This integration enables an efficient response to emergencies by facilitating real-time interaction and control of robots remotely.

Furthermore, Lim (2019) explored the integration of ROS with cloud computing infrastructure to offload computationally intensive tasks and enhance scalability. They utilized RWT to develop web-based visualization tools for analyzing sensor data in real-time, showcasing its versatility in cloud robotics applications.

2.5 Synthesis of the Study

The conducted review of related literature provides a comprehensive overview of existing methods, techniques, and technologies used for volume measurement, point cloud acquisition devices, and volume measurement using 3D point cloud data. It highlights the importance of enhancing

post-harvest processing and storage technology to meet increasing global demand and minimize waste, emphasizing the role of advanced monitoring and management techniques in improving production efficiency and safety standards.

Various methods for volume measurement, including traditional level measurements and emerging technologies such as LiDAR, have been discussed. While traditional methods like weighted fiberglass tape provide a single data point, newer technologies offer more detailed and accurate measurements. Point cloud acquisition devices, particularly LiDAR, have emerged as powerful tools for generating detailed 3D models of objects or environments. Techniques for transforming 2D LiDAR scanners into 3D point cloud scanners have been explored, highlighting the use of rotating mechanisms and processing algorithms.

Additionally, the review discusses frameworks for point cloud processing, visualization, and mapping, emphasizing the importance of utilizing tools like ROS and PCL for efficient data handling. Techniques and methods for volume estimation using computational geometry, such as Delaunay triangulation and voxelization, have been examined, along with their applications in various industries.

Furthermore, the integration of Robot Web Tools (RWT) with ROS for remote monitoring of robots has been explored, demonstrating its potential in enabling real-time interaction and control of robots over the web. Several

studies have demonstrated the capabilities of RWT in disaster management, cloud robotics, and real-time sensor data analysis.

Given the advancements in point cloud acquisition devices, volume measurement techniques, and web-based robotics interfaces, this study focused on integrating and utilizing these technologies and methods to provide an alternative solution to existing technology used in storage volume calculation. By leveraging existing technologies and methodologies, the aim of this study was to develop a feasible approach for enhancing storage technology especially in volume measurement technology.

CHAPTER III

METHODOLOGY

In this chapter, the study discusses the systematic approach employed in the development of of the proposed system. As depicted in Figure 3.1, each phases is essential in shaping the overall system functionality. This chapter explains the approach taken, giving an overview of the techniques, methods, and resources applied at every development step.
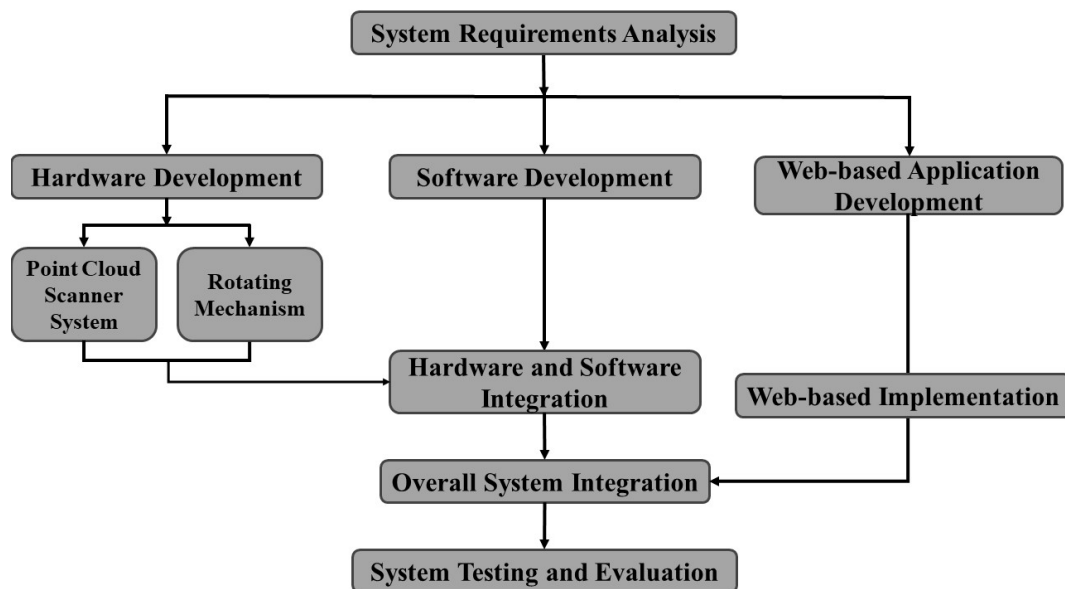

Figure 3.1. System Development Process

3.1   System Requirements Analysis

The development process of the study encompasses hardware, software, and web-based application design, followed by system integration and testing. As depicted in Figure 3.2 which is the proposed overall system setup, the study undertook the design and development of two distinct yet interconnected systems: the 3D Point Cloud Scanner (3D-PCSS), which is placed at the top of a storage bin, and the web-based application which is both connected to the local network. This overall system setup achieved by following a step by step development process which is illustrated in figure 3.1, identifying hardware aspect which involves selecting and configuring the necessary components for data acquisition, processing, and communication. software development focuses on programming the processes to control hardware functionality and execute specific tasks. Meanwhile, web-based application design requires creating an interface for users to interact and data visualization. System integration involves bringing together these components and ensuring communication and functionality between them. Lastly, system testing and evaluation was conducted to validate the functionality, performance, and reliability of the developed systems through various testing procedures.
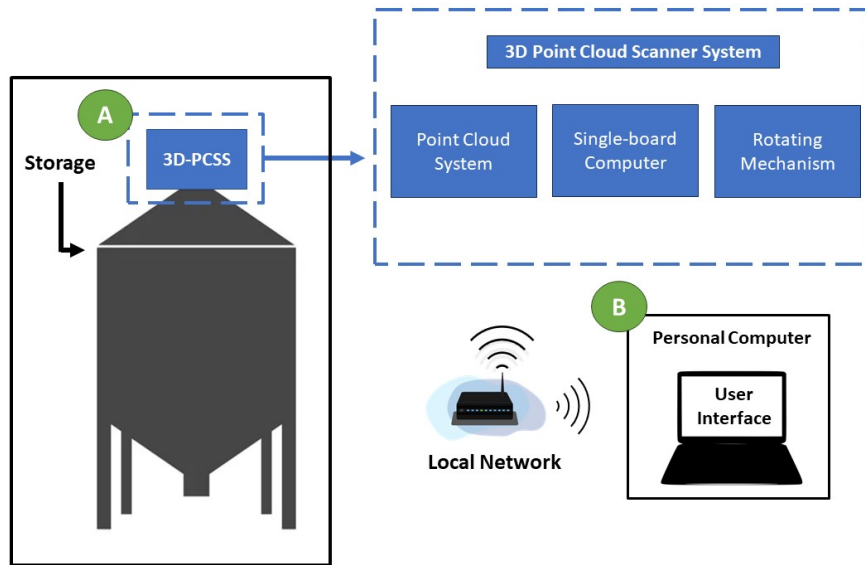
Figure 3.2. Overall System Setup: (A) 3D-PCSS, (B) User Interface

3.2 Hardware Development

The hardware development conducted in this study involves the design and construction of 3D point cloud scanner. The system is divided in to two parts which discussed in the following subsection.

3.2.1 3D Point Cloud Scanner Design (3D-PCSS)

The 3D-PCSS in this study considers the following design and functionality:

- Based on low-cost 2D LiDAR device.

- Compact and portable for simplified installation.

- Support for connecting to a local network for remote data visualization and monitoring.

- Utilizing Robot Operating System (ROS) and Point Cloud Library (PCL) for adaptability development.

To achieve the design and functionality of the system mentioned, the development process, components and integration is discussed in the following section

Point Cloud Scanner System

Point cloud devices, such as LiDAR (Light Detection and Ranging), offer exceptional accuracy in acquiring distance measurements over considerable distances. LiDAR systems emit laser pulses and measure the time it takes for these pulses to return after bouncing off objects in the environment. This technology enables the creation of highly detailed and accurate three-dimensional point clouds, which represent the surfaces and structures within the scanned area. Even low-cost LiDAR options are available in the market, making this technology accessible for various applications and budgets.

The point cloud scanner system in this study used a low-cost 2D LiDAR device controlled with single-board computer (SBC) for its computing functionality.

Rotating Mechanism

The rotating mechanism design which is attached to the 2D LiDAR in this study is based on the methodology outlined in a previous research conducted by Clar and Salaan (2022). This prior study served as a foundational framework for the development of the rotating 2D LiDAR system in this study, providing into the integration of a pan-tilt unit (PTU) with a 2D LiDAR scanner to enable three-dimensional point cloud scanning. By employment the principles and techniques conducted in Clar and Salaan (2022), the current study aims to further refine and enhance the performance of the rotating 2D LiDAR system for its intended application and also address the problem encountered in the previous study.

The servo motor used in this study is compatible with a Software Development Kit (SDK) that includes configurations for integration with the Robot Operating System (ROS). This compatibility allows for communication and control of the servo motor within the ROS environment, facilitating the development of flexible and efficient robotic systems.

By employing this feature, the LiDAR and servo can communicate and synchronize. Figure 3.4 illustrates how the servo is attached to the 2D LiDAR device to add an additional axis of movement. The figure also depicts the respective scan angle directions of the LiDAR and the movement direction servo motor.

Synchronization is a crucial aspect of this process. The synchronization method developed in this study is detailed in Figure 3.3.
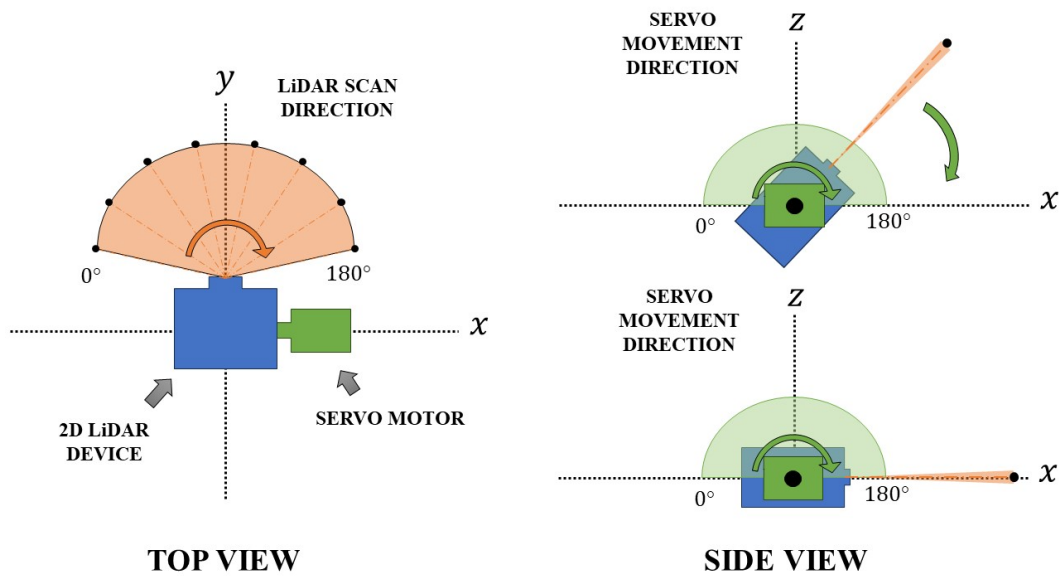

Figure 3.3. Scan Direction of LiDAR and Movement Direction of the Servo
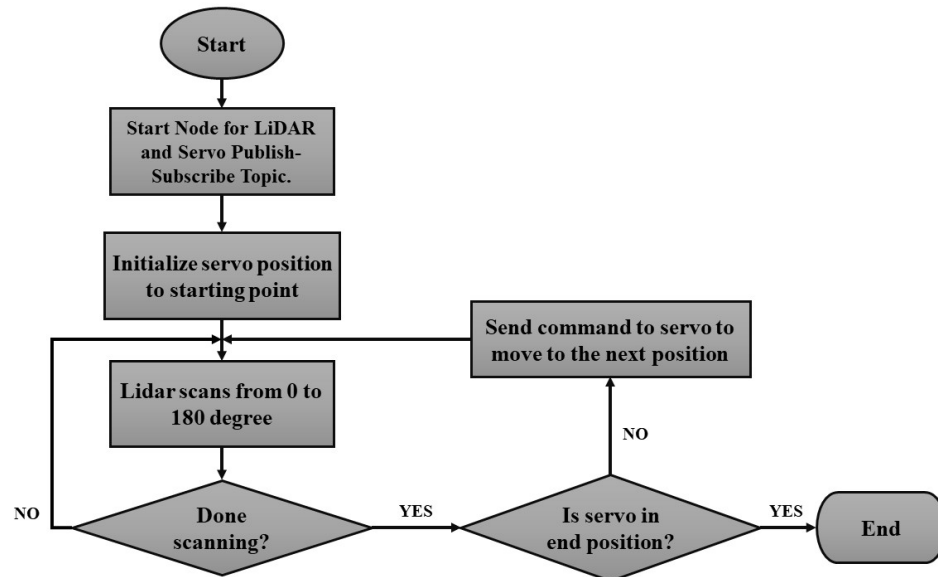

Figure 3.4. Synchronization Process of LiDAR and Servo

In figure 3.5, the components of the point cloud scanner and rotating

device are integrated to develop a 3D point cloud scanner system. These individual components are divided into four categories, as shown in figure 3.6: sensor, control, actuator, and power. The double-headed arrow indicates a two-way communication from and to the control device. Lastly, the hardware design flow chart of the system is shown in figure 3.7.
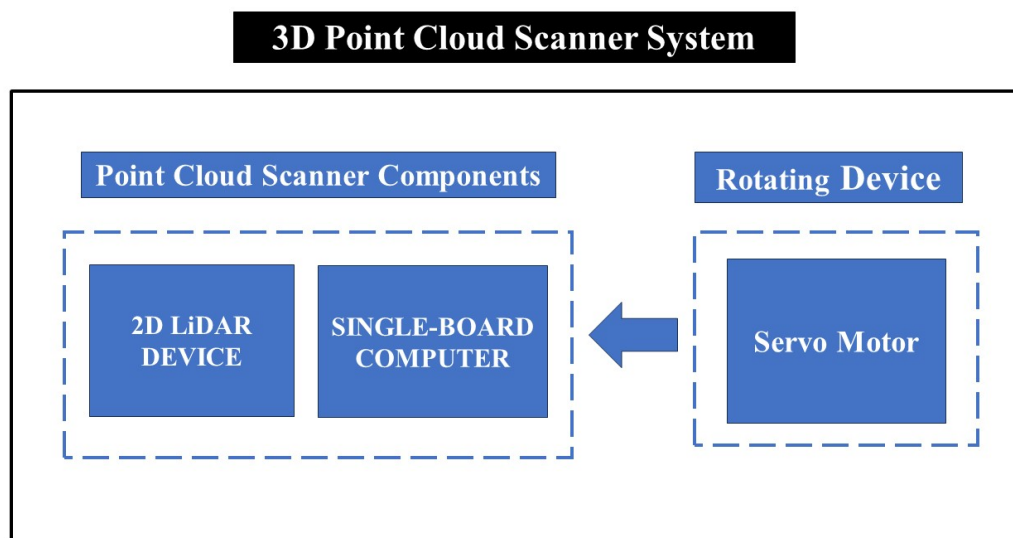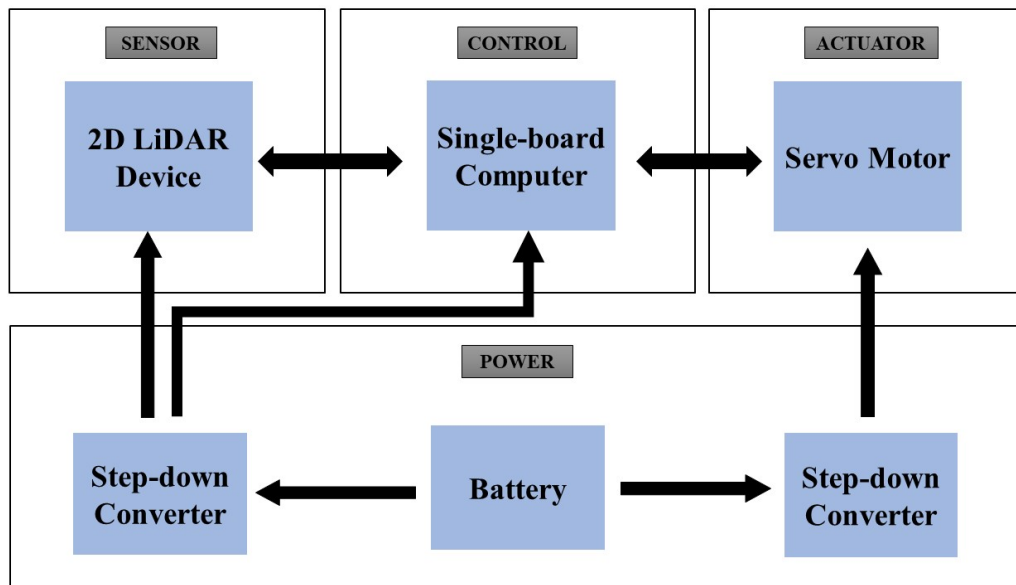
Figure 3.5. Major Components of 3D-PCSS

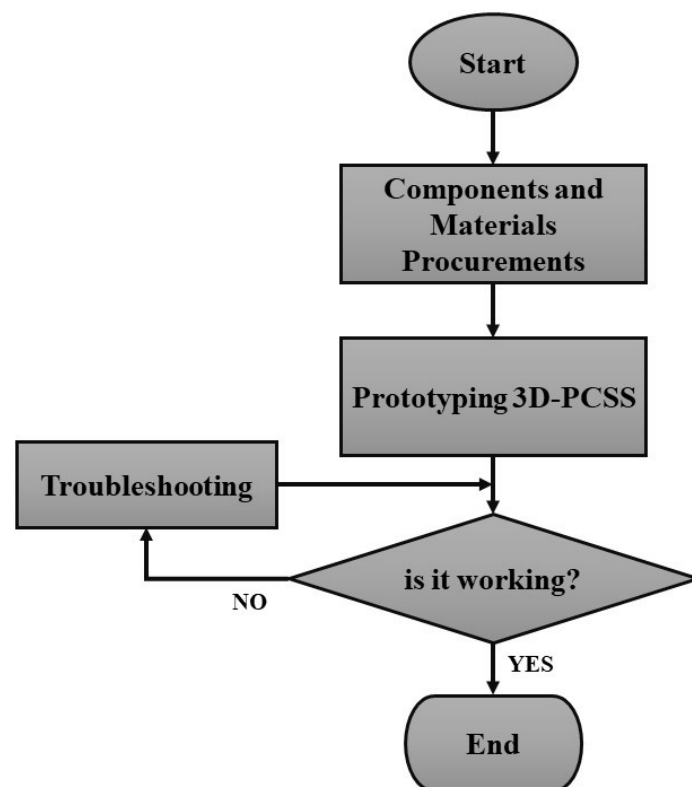**Figure 3.6.** Block Diagram Connection of the Components

Figure 3.7. Hardware Design Flow Chart

3.3 Software Development

Software design plays a crucial role in the development of the 3D-PCSS by facilitating communication between hardware components, and allows connection with external software system. The system was designed to initialize all necessary components, including nodes and connection, immediately upon power-up. This ensures seamless operation and also establish connection with the developed web application for user interaction. As described in figure 3.8, after turning on the system, it initializes essential nodes and enter in idle mode waiting for an external command coming from the web application. The system remain in idle mode unless turnoff. The development of software processes, including the choice of operating system and frameworks is outlined in this section.

Throughout this study, it's important to note that the terms 'process' and 'nodes' are used interchangeably. This interchangeable usage highlights the fundamental concept in ROS where processes, represented as nodes, perform computation and communication tasks within the system.
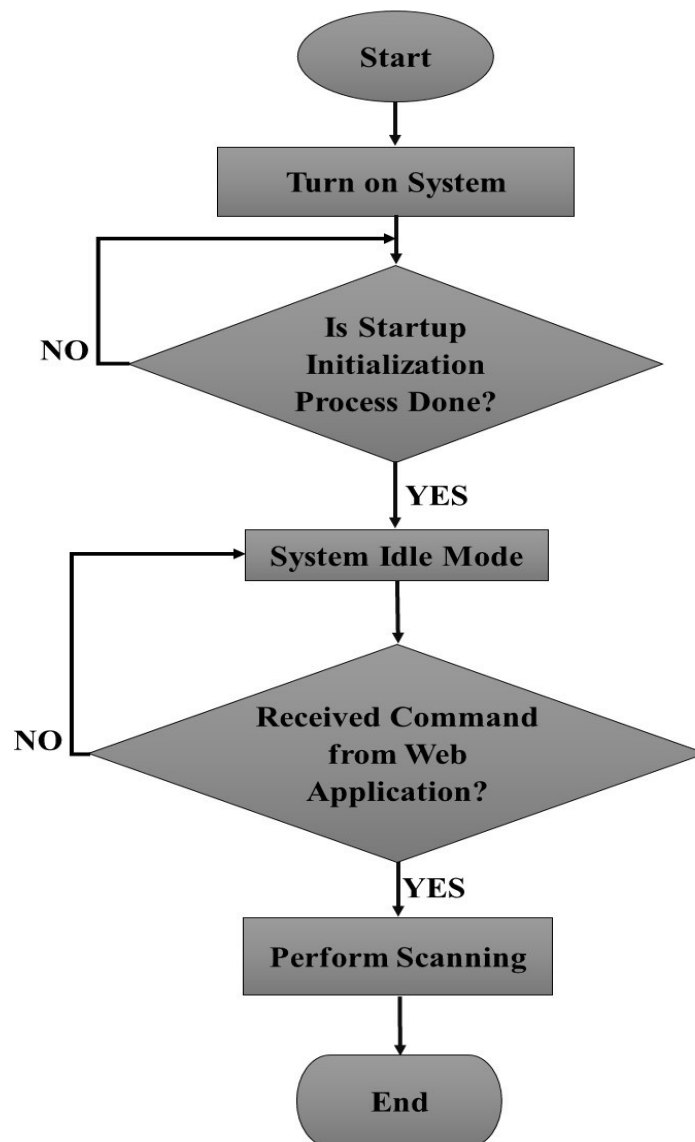
Figure 3.8. System Idle Mode Process Flow Chart

3.3.1 Operating System and Frameworks

In this study, the single-board computer (SBC) used in the 3D-PCSS requires an appropriate OS and frameworks to support the execution of firmware and software components. Linux-based operating systems, such

as Ubuntu, is commonly chosen for SBCs due to its reliability, flexibility, and extensive community support. This OS option provide a stable platform for running Robot Operating System (ROS) nodes and managing system resources effectively, thus, was utilized in this study. ROS framework was also utilized in this study to develop a publish-subscribe relationship between ROS nodes. Lastly, Point Cloud Library (PCL) serves in this study as a fundamental library being used for processing and analyzing point cloud data. PCL provides a comprehensive set of algorithms and tools for tasks such as point cloud registration, filtering and computational geometry to name a few.

3.3.2   Startup Initialization Process

Roscore and rosgridge are the two essential cores that used in the software of 3D-PCSS. These cores or nodes typically need to be executed manually through the command-line interface (CLI) or desktop environment terminal to run and process data, or to initiate other nodes and do specific tasks. However, it is impractical to start and stop this nodes each time the system is turn on or off, thus, in this study a custom service file was developed to automate and start these nodes after the system is turn on. This file is created using Linux systemd to configure and instantly run the cores.

3.3.3 System Scanning and LiDAR Range Values Processes

As described in figure 3.2, the system is placed at the top of the storage bin. Once the system receive a command from the web application, it will start scanning the inside of the storage bin and acquiring ranges values from the LiDAR as discussed in figure 3.8. The study developed a ros nodes that handle different processes such as initialization of the LiDAR device and servo motor, establishing a publish-subscribe relationship between these devices, and the conversion of LiDAR range scan data to point cloud data. The raw scan data from the LiDAR are typically range values of the return pulses. These range values enters different stages of pre-processes to be mapped in two- or three-dimensional Euclidean space to create a point cloud data and use for further post-processing. The flow of the processes from initialization to mapped point cloud data is illustrated in this figure 3.9 The method used in this study for processing the ranges values gathered from the LiDAR device is described in the figure 3.10. ρ translates to the distance from the origin $(0,0,0)$, which is the in our case the LiDAR, and this distance is measured as meter. The angle θ is the rotation around the z-axis in the xy-plane. The angle ϕ is the tilt of the radius vector from the positive z-axis, it goes from 0 degree at the positive z-axis down to 90 degree at the xy-plane and all the way down to 180 degree on the negative z-axis. Equation 3.1, 3.2 and 3.3 shows the X, Y, and Z conversion formula

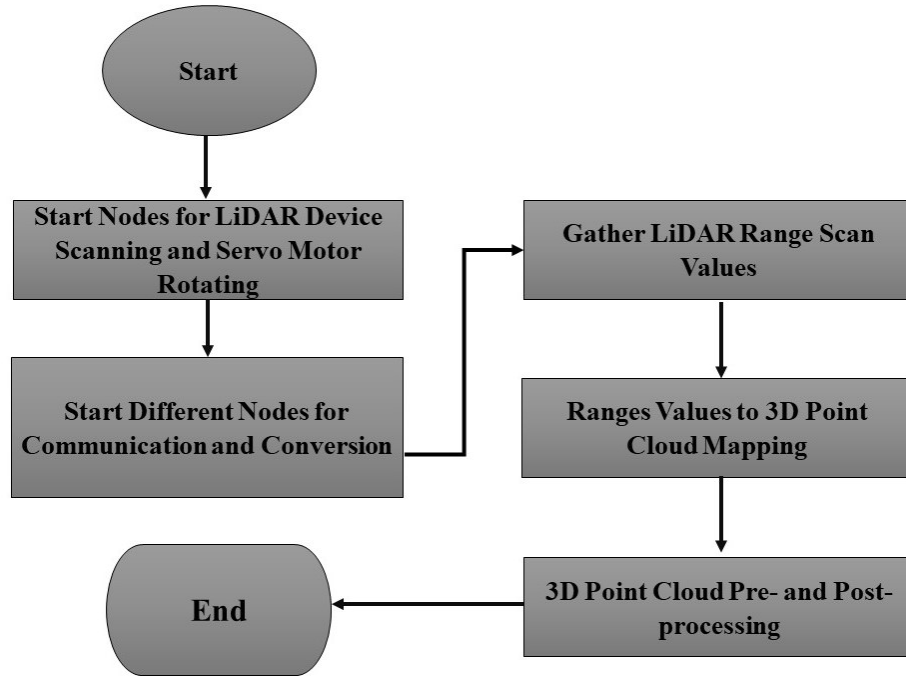respectively.

Figure 3.9. From Scanning to Mapped Point Cloud Data Flow Chart

$$x = \rho \times \sin(\theta) \times \cos(\phi) \tag{3.1}$$

$$y = \rho \times \sin(\theta) \times \sin(\phi) \tag{3.2}$$

$$z = \rho \times \cos(\theta) \tag{3.3}$$
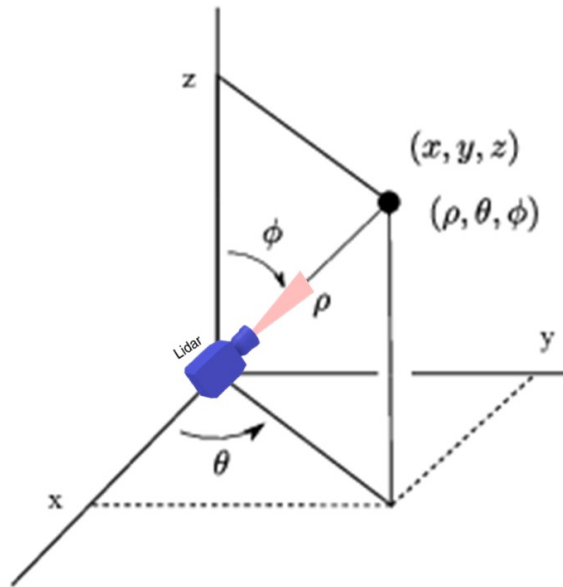
Figure 3.10. LiDAR Scan Range Conversion from Polar Coordintes (ρ, θ, ϕ), to Cartesian Coordinate (x, y, z)

3.3.4 Point Cloud Data to Measured Volume

An Empty-space approached was used to measured the flour materials inside the storage bin. A simple representation of an empty-space approach is illustrated in figure 3.11. The 3D-PCSS is place at the top of the storage bin to scan the empty space and generate point cloud data. These point cloud data is process to calculate the the empty space volume using Convex Hull method. Theoretically, the volume of the flour materials is determined by subtracting the empty space volume from the bin's maximum volume capacity as it is also a commonly used method in these studies Raba et al. (2020); Clar and Salaan (2022).
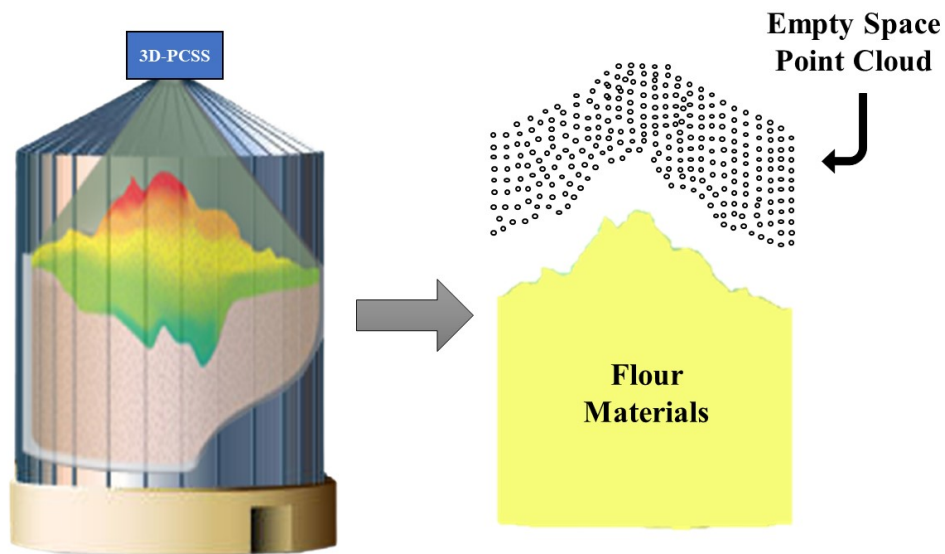
Figure 3.11. System Scanning (right), Generated Empty Space Point Cloud
Data (left)

3.4 Web-based Application Development

This section covers the process of developing the custom user interface
for the 3D-PCSS utilizing web application. The flow of the connection of the
web application connecting to the 3D-PCSS is presented in the figure 3.12.
The system and the web application is within the same local network, thus
after entering the local and port address in the web application, the web
socket connection can be established and can send command to the system.

The user interface consider the following design and functionality, the
UI should be:

- Intuitive and simple.

- Able to establish connection to the 3D-PCSS.

- Able to send command, display 3D point cloud data and volume measurement.

Figure 3.12. Web Application Connection Process Flow Chart

3.4.1 Communication Protocol

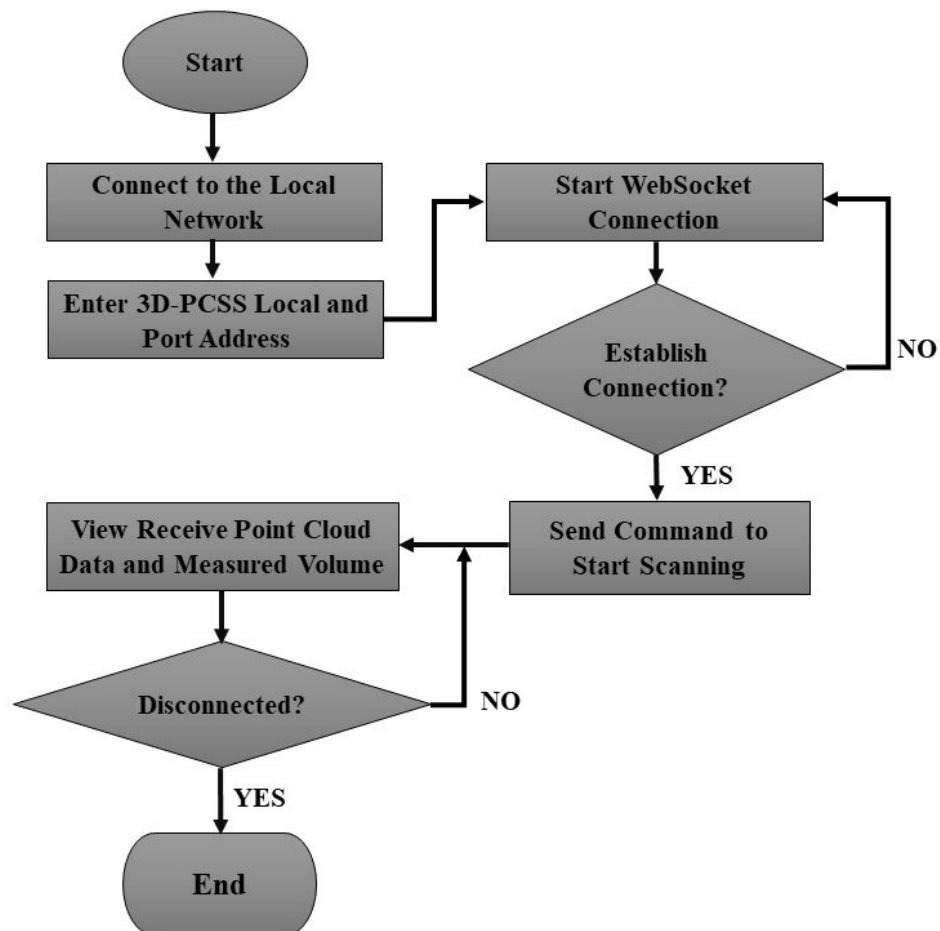The web-based interface and 3D-PCSS utilizes WebSocket communication protocol. This communication uses full-duplex channels to establish over a single TCP connection. It allows for less latency than typical HTTP

connections when a client and server interact. Within the framework of ROS applications, WebSocket enables bi-directional, real-time communication, enabling servers to rapidly transmit updates to clients. The figure 3.13 demonstrate the initialization of the Websocket communication between the web interface and the 3D-PCSS. The following step to establish this communication is explain below:

1. **The Client Makes a Request:** The WebSocket client initiates the handshake by sending an HTTP request to the server.

2. **The Server Accepts the Request:** If the server is willing to establish a WebSocket connection, it responds with an HTTP response that has a status code of 101 (Switching Protocols).

3. **WebSocket Connection Established:** Once both the client and server have exchanged their handshake messages, the WebSocket connection is established. Data can now flow bidirectionally between the client and server over the single TCP connection.
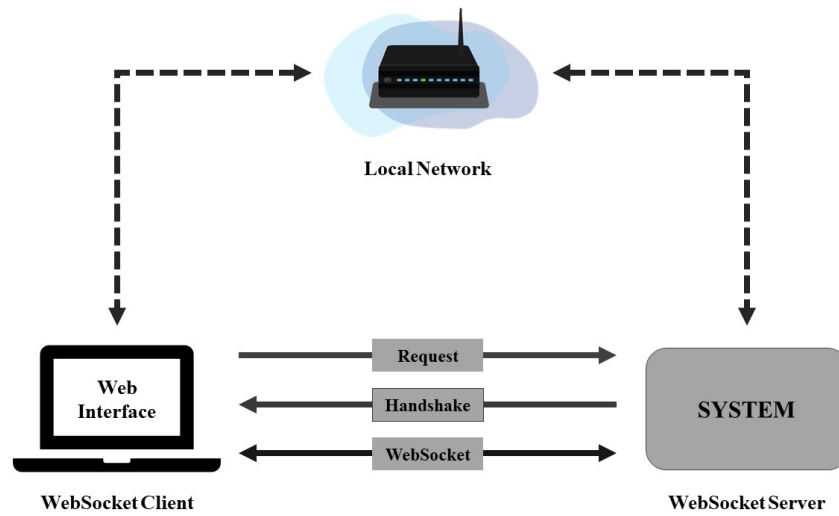
Figure 3.13. Communication Protocol of the Web Interface and the System

3.5 Overall System Testing and Evaluation

In this section, various tests were conducted to evaluate the performance of the overall system. After successful development and integration of the system and web application, they were tested and evaluated for accuracy and functionality.

3.5.1 Constructing of Storage Bin

To test the performance and accuracy of the overall system, the study involves constructing a mock-up flour storage bin modeled after those commonly used in food manufacturing industries. The mock-up bin is designed to closely mimic the geometric shape and proportions of real storage bins used in practice. The CAD model design, shown in figure 3.14, serves as the

guide for the physical construction. The design is composed of rectangular shape and conical frustum underneath. The CAD design of rectangular shape has a dimension of 2.5 meters in height, 0.5 meters in length, and 0.69 meters in width. The conical frustum, which is tapers from the base of the rectangular section, has a top radius of 0.21 meters, a bottom radius of 0.17 meters and height of 0.21 meters. The 3D-PCSS was placed at the top of created mock-up storage bin for test and evaluation.
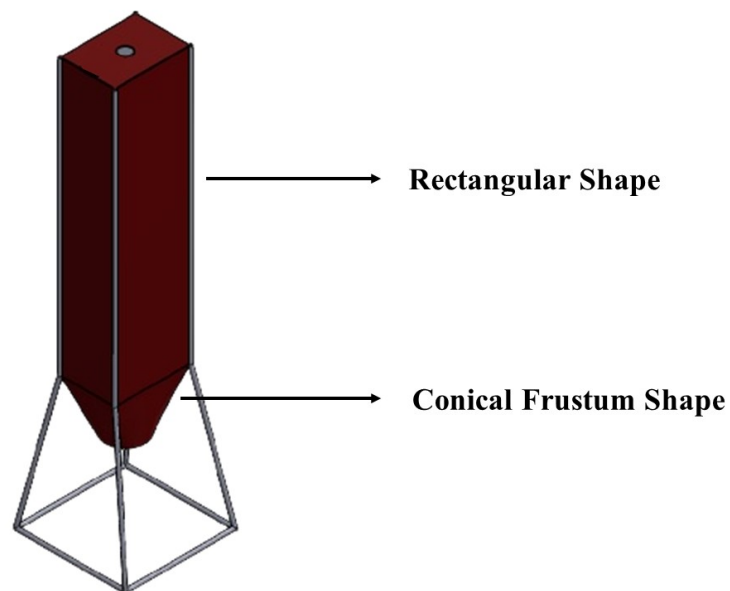

Figure 3.14. CAD Model Design of the Storage Bin

3.5.2 Different Testing Case Procedure

The study conducted different tests and evaluations to observe the accuracy and performance of the overall system. The study performed multiple tests to assess and validate the accuracy and effectiveness of the developed method, and each of tests had multiple trials. The different testing

procedures of the system were as follows:

Test Case 1: Empty Storage Bin Scanning

In this test case, multiple scans of an empty storage bin were conducted. This involved performing 30 or more scanning trials. By comparing the system's measured volume with the actual volume capacity of the storage bin, the test aimed to validate the overall system's performance and accuracy. This test also provided a baseline for assessing the performance of the developed method.

Test Case 2: Filling the Storage Bin with Known Volume

The second test case involved filling the storage bin with flour using containers of known volume. Three specific scenarios were conducted, each with different percentages of the storage bin's maximum capacity, along with known volumes and two different flour surface contour:

1. The storage bin was filled up to 5.8% of its maximum capacity, with a known volume of 0.0594 cubic meters.

2. The storage bin was filled up to 47.2% of its maximum capacity, with a known volume of 0.4752 cubic meters.

3. The storage bin was filled up to 70.37% of its maximum capacity, with a known volume of 0.7128 cubic meters.

These different test cases were designed to assess the accuracy and performance of the overall system.

CHAPTER IV

RESULT AND DISCUSSION

The results of the system development outlined in the previous chapter were presented and discussed in this chapter. After evaluating the specification of each system and undergo different design revision and integration, the study successfully identified and finalized the necessary components, tools and materials for each system.

4.1 Developed 3D Point Cloud Scanner System (3D-PCSS)

4.1.1 3D-PCSS CAD Design Setup

The 3D Point Cloud Scanner System hardware setup, as shown in Figure 4.1, consists of a 2D LiDAR Device fixed to a platform connected to a servo motor. This servo motor allows the platform to rotate, giving the LiDAR device an extra axis of movement. Inside the compartment is where the single-board computer along with other circuit components located. The detailed specification of each of the components is presented in appendix A.
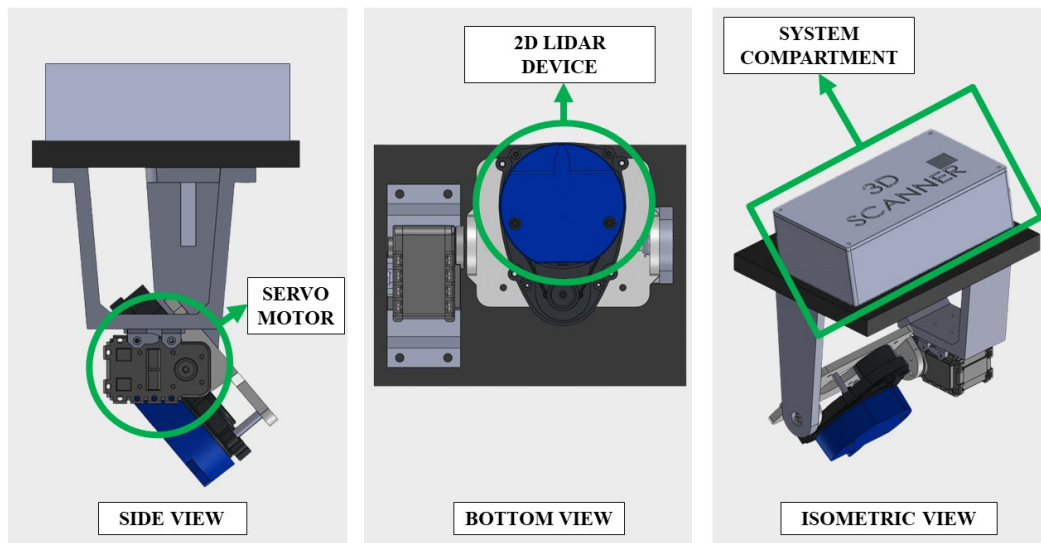
Figure 4.1. Different View of the CAD Model Design of 3D-PCSS

4.1.2 Actual Design of the 3D-PCSS

The actual development of the 3D-PCSS shown in figure 4.2 was constructed in accordance with the 3D CAD model design and the system is powered by a battery. The base platform, to which the 2D LiDAR device and servo motor are attached, was fabricated using aluminum metal. The system compartment is fabricated using a 3D printer and employing ABS material. Inside the compartment, the specific components and its category is shown in figure 4.3

Figure 4.2. Actual 3D-PCSS Developed
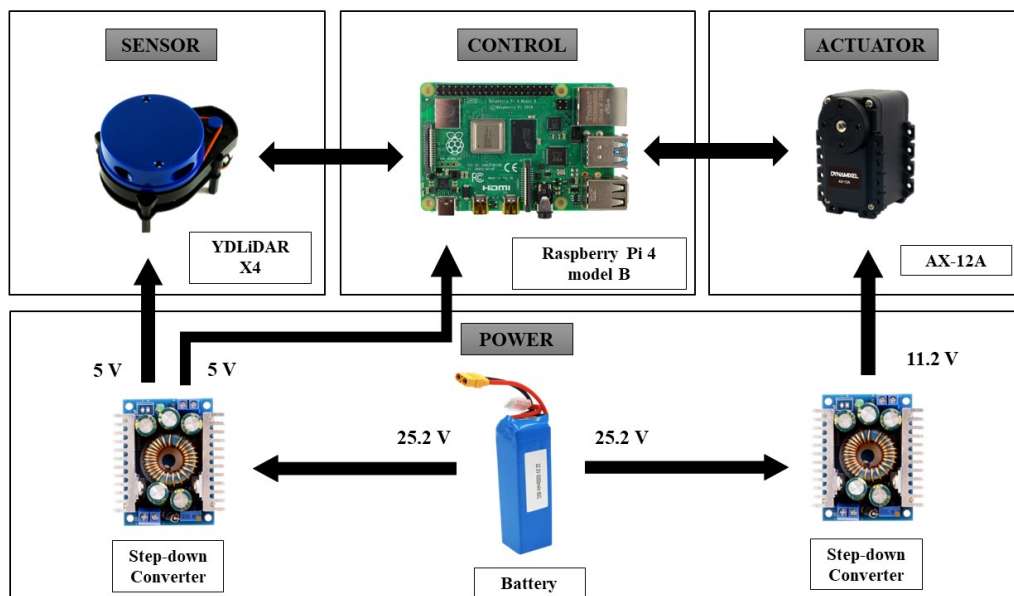
Figure 4.3. Specific Components of the System

4.2 Software Implementation

The processes discussed in the previous chapter were implemented on the single-board computer (Raspberry Pi), playing a crucial role in the overall functionality of the 3D-PCSS. Figure 4.4 illustrates the various nodes, topics, and their relationships in a publish-subscribe model. The arrows in the diagram show how data flows between the different nodes and its relationship to a corresponding topics. The ROS bridge server Node facilitates communication by relaying commands between the web application and the ROS framework via the "/rosapi" service. Commands to start and stop scanning from the web interface are processed using the Remote Command Node within the system. The LiDAR Node captures data and publishes it as range values, while the Dynamixel Node and LiDAR Node synchronize their operations through the "/dxl_pos" topic. The Scan to 3D Point Cloud Mapping Node converts raw scan data into usable 3D point cloud data. Finally, the post-processing stage refines the point cloud data for volume measurement.

Figure 4.4. Try

4.3 Web-based User Interface Implementation

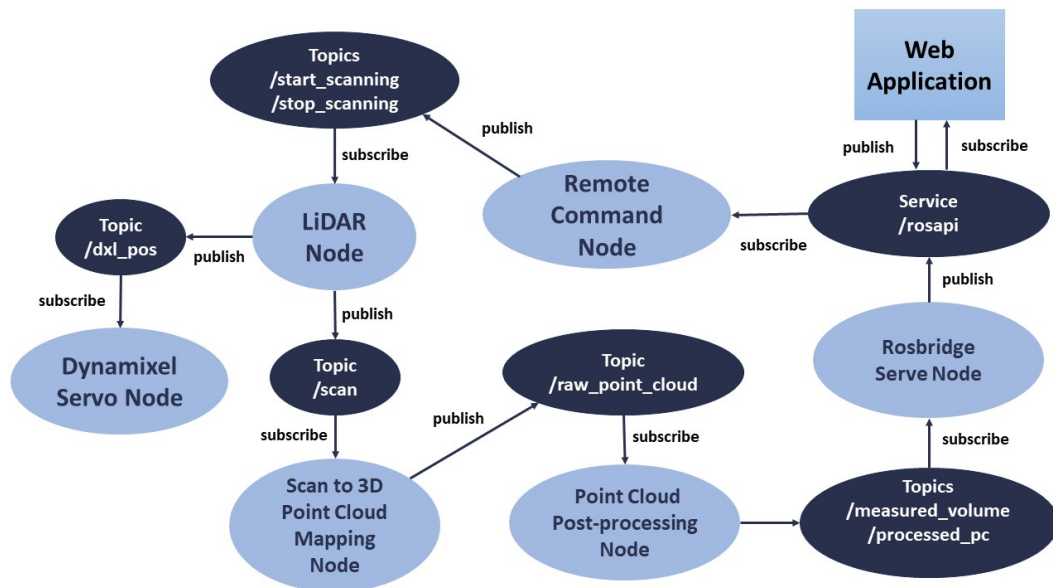A variety set of tools and frameworks were employed to enhance the functionality of the Web Interface. Table 4.1 outlines the various tools, frameworks, and libraries utilized in the implementation of the web-based user interface.

Table 4.1. Tools and Frameworks Used in the Web-based User Interface

Tool/Framework	Description/Functionality
jQuery	Used for simplifying JavaScript programming and DOM manipulation, jQuery is included via CDN for easy integration.
Three.js	This JavaScript library is utilized for rendering 3D graphics in a web browser. It enables the display of the 3D point cloud viewer within the application.
EventEmitter2	EventEmitter2 is employed for implementing event-driven programming, allowing efficient communication between different components of the application.
roslib.js	roslib.js is utilized for connecting the web application to the Robot Operating System (ROS), enabling communication with ROS nodes and topics.
Bootstrap	The Bootstrap framework is employed for responsive design and styling of the user interface components. It ensures consistency and enhances the visual appeal of the application.
Chart.js	This JavaScript library is used for creating interactive charts and graphs to visualize data. It enhances the user experience by providing intuitive data representation.
ros3d.js	ros3d.js is utilized for integrating ROS visualization capabilities into the web application. It facilitates the display of ROS topics such as point clouds and robot models.

These tools and frameworks collectively contribute to the functionality of the web-based user interface for the 3D-PCSS.

BIBLIOGRAPHY

Auat Cheein, F. A., Guivant, J., Sanz, R., Escolà, A., Yandún, F., Torres-Torriti, M., and Rosell-Polo, J. R. (2015). Real-time approaches for characterization of fully and partially scanned canopies in groves. *Computers and Electronics in Agriculture*, 118:361–371.

Barber, C. B., Dobkin, D. P., and Huhdanpaa, H. T. (1996). The quickhull algorithm for convex hulls. *ACM Transactions on Mathematical Software (TOMS)*, 22(4):469–483.

Bewley, A., Shekhar, R., Leonard, S., Upcroft, B., and Lever, P. (2011). Real-time volume estimation of a dragline payload. In *2011 IEEE International Conference on Robotics and Automation*, pages 1571–1576.

Bi, S., Yuan, C., Liu, C., Cheng, J., Wang, W., and Cai, Y. (2021). A survey of low-cost 3d laser scanning technology. *Applied Sciences*, 11(9).

Bucklin, R., Thompson, S., Montross, M., and Abdel-Hadi, A. (2019). Chapter 9 - grain storage systems design. In Kutz, M., editor, *Handbook of Farm, Dairy and Food Machinery Engineering (Third Edition)*, pages 175–223. Academic Press, third edition edition.

Bulut, S., Giese, T. G., Wende, M., and Anderl, R. (2020). The paperless factory: From document driven factories to model driven factories. In

2020 IEEE International Conference on Teaching, Assessment, and Learning for Engineering (TALE), pages 725–730.

Chan, T. (1996). Optimal output-sensitive convex hull algorithms in two and three dimensions. *Discrete & Computational Geometry*, 16(4):361–368.

Chang, W.-C., Wu, C.-H., Tsai, Y.-H., and Chiu, W.-Y. (2017). Object volume estimation based on 3d point cloud. In *2017 International Automatic Control Conference (CACS)*, pages 1–5.

Chua, C. K., Wong, C. H., and Yeong, W. Y. (2017). Chapter four - software and data format. In Chua, C. K., Wong, C. H., and Yeong, W. Y., editors, *Standards, Quality Control, and Measurement Sciences in 3D Printing and Additive Manufacturing*, pages 75–94. Academic Press.

Clar, S. E. and Salaan, C. J. O. (2022). Volume estimation using convex hull method for point cloud-based materials inside a silo.

Duff, E. (2000). Automated volume estimation of haul-truck loads.

Duysak, H. and Yigit, E. (2020). Machine learning based quantity measurement method for grain silos. *Measurement*, 152:107279.

Graham, R. L. and Frances Yao, F. (1983). Finding the convex hull of a simple polygon. *Journal of Algorithms*, 4(4):324–331.

Guevara, J., Arevalo-Ramirez, T., Yandun, F., Torres-Torriti, M., and Cheein,

F. A. (2020). Point cloud-based estimation of effective payload volume for earthmoving loaders. *Automation in Construction*, 117:103207.

Jaboyedoff, M., Oppikofer, T., Abellán, A., Derron, M.-H., Loye, A., Metzger, R., and Pedrazzini, A. (2012). Use of lidar in landslide investigations: a review. *Natural Hazards*, 61(1):5–28.

Jeong, D., Li, Y., Lee, H. J., Lee, S. M., Yang, J., Park, S., Kim, H., Choi, Y., and Kim, J. (2018). Efficient 3d volume reconstruction from a point cloud using a phase-field method. *Mathematical Problems in Engineering*, 2018:7090186.

Kang, X., Yin, S., and Fen, Y. (2018). 3d reconstruction & assessment framework based on affordable 2d lidar. In *2018 IEEE/ASME International Conference on Advanced Intelligent Mechatronics AIM*, pages 292–297.

Kim, Y. (2002). Convex hull ensemble machine. In *2002 IEEE International Conference on Data Mining, 2002. Proceedings.*, pages 243–249.

Kumar, D. and Kalita, P. (2017). Reducing postharvest losses during storage of grain crops to strengthen food security in developing countries. *Foods*, 6(1).

Lim, J. Z. (2019). *Cloud Based Ros Implementation for Indoor Robot*. PhD thesis, UTAR.

Liu, Y. and Zheng, Y. (2021). Accurate volume calculation driven by

delaunay triangulation for coal measurement. *Scientific Programming*, 2021:6613264.

Maus, A. (1984). Delaunay triangulation and the convex hull ofn points in expected linear time. *BIT Numerical Mathematics*, 24(2):151–163.

Meng, X., Wang, T., Cheng, D., Su, W., Yao, P., Ma, X., and He, M. (2023). Enhanced point cloud slicing method for volume calculation of large irregular bodies: Validation in open-pit mining. *Remote Sensing*, 15(20).

Munarso, S. J., Widayanti, S. M., and Qanytah (2022). Advances in postharvest technology and its implementation. *IOP Conference Series: Earth and Environmental Science*, 1024(1):012001.

Ocando, M. G., Certad, N., Alvarado, S., and Terrones, Á. (2017). Autonomous 2d slam and 3d mapping of an environment using a single 2d lidar and ros. In *2017 Latin American Robotics Symposium (LARS) and 2017 Brazilian Symposium on Robotics (SBR)*, pages 1–6.

Putman, E. B. and Popescu, S. C. (2018). Automated estimation of standing dead tree volume using voxelized terrestrial lidar data. *IEEE Transactions on Geoscience and Remote Sensing*, 56(11):6484–6503.

Qureshi, B., Koubaa, A., Sriti, M.-F., Javed, Y., and Alajlan, M. (2016). Poster: Dronemap-a cloud-based architecture for the internet-of-drones. In *EWSN*, pages 255–256.

Raba, D., Gurt, S., Vila Clarà, O., and Farrés, E. (2020). An internet of things (iot) solution to optimise the livestock feed supply chain. pages 103–118.

Raj, T., Hashim, F., Huddin, A., Ibrahim, M. F., and Hussain, A. (2020). A survey on lidar scanning mechanisms. *Electronics*, 9:741.

Rhee, J. H., Kim, S. I., Lee, K. M., Kim, M. K., and Lim, Y. M. (2021). Optimization of position and number of hotspot detectors using artificial neural network and genetic algorithm to estimate material levels inside a silo. *Sensors*, 21(13).

Rusu, R. B. and Cousins, S. (2011). 3d is here: Point cloud library (pcl). In *2011 IEEE International Conference on Robotics and Automation*, pages 1–4.

Sarker, V. K., Qingqing, L., and Westerlund, T. (2020). 3d perception with low-cost 2d lidar and edge computing for enhanced obstacle detection. In *2020 IEEE Conference on Industrial Cyberphysical Systems (ICPS)*, volume 1, pages 49–54.

St-Onge, D. and Herath, D. (2022). *The Robot Operating System (ROS1 &2): Programming Paradigms and Deployment*, pages 105–126. Springer Nature Singapore, Singapore.

Stojanovic, V. (2023). Point cloud analytics: Proposed future work. *Proceedings of the HPI Research School on Service-oriented Systems Engineering 2020 Fall Retreat*, page 137.

Turner, A., Jackson, J., Koeninger, N., Mcneill, S., Montross, M., Casada, J., Boac, R., Bhadra, R., Maghirang, S., and Thompson (2017). Stored grain volume measurementusing a low density point cloud. *Applied Engineering in Agriculture*, 33:105–112.

Turner, A., Jackson, J., Koeninger, N., Mcneill, S., Montross, M., Casada, M., Boac, J., Bhadra, R., Maghirang, R., and Thompson, S. (2016). Error analysis of stored grain inventory determination. *Transactions of the ASABE (American Society of Agricultural and Biological Engineers)*, 59:1061–1072.

Vogt, M. and Gerding, M. (2017). Silo and tank vision: Applicaltions, challenges, and technical solutions for radar measurement of liquids and bulk solids in tanks and silos. *IEEE Microwave Magazine*, 18(6):38–51.

Wang, Q. and Kim, M.-K. (2019). Applications of 3d point cloud data in the construction industry: A fifteen-year review from 2004 to 2018. *Advanced Engineering Informatics*, 39:306–319.

Yegorova, S. V., Slavyanskiy, A. A., Postnikova, T. A., Pereboev, A. V., Mazanova, G. V., and Murzakov, M. G. (2021). Improving the technology of post-harvest processing and storage of grain raw materials at the enterprises of the grain processing industry. *IOP Conference Series: Earth and Environmental Science*, 640(2):022040.

Yigit, E., İsiker, H., Toktas, A., and Tjuatja, S. (2015). Cs-based radar mea-

surement of silos level. In *2015 IEEE International Geoscience and Remote Sensing Symposium (IGARSS)*, pages 3746–3749.

Yuan, C., Bi, S., Cheng, J., Yang, D., and Wang, W. (2021). Low-cost calibration of matching error between lidar and motor for a rotating 2d lidar. *Applied Sciences*, 11(3).

Zhi, Y., Zhang, Y., Chen, H., Yang, K., and Xia, H. (2016). A method of 3d point cloud volume calculation based on slice method. In *Proceedings of the 2016 International Conference on Intelligent Control and Computer Application*, pages 155–158. Atlantis Press.

APPENDIX A

COMPONENTS SPECIFICATION

YDLiDAR Model X4

1 PRODUCT OVERVIEW

YDLIDAR X4 is a 360 degrees 2D LiDAR (hereinafter referred to as X4) developed by EAI team. Based on the principle of triangulation, it is equipped with related optics, electricity, and algorithm design to achieve high-frequency and high-precision distance measurement. The mechanical structure rotates 360 degrees to continuously output the angle information as well as the point cloud data of the scanning environment while ranging.

1.1 Product Features

➢ 360 degrees scan ranging
➢ High accuracy, stable performance
➢ Wide measuring range
➢ Strong resistance to ambient light interference
➢ Low power consumption, small size, stable performance and long service life
➢ Class I eye safety
➢ Motor speed is adjustable, the proposed speed is 6~12Hz
➢ High-speed ranging, ranging frequency up to 5kHz

1.2 Applications

➢ Robot navigation and obstacle avoidance
➢ Robot ROS teaching and research
➢ Regional security
➢ Environmental scanning and 3D reconstruction
➢ Navigation and obstacle avoidance of home robots/ robot vacuum cleaners
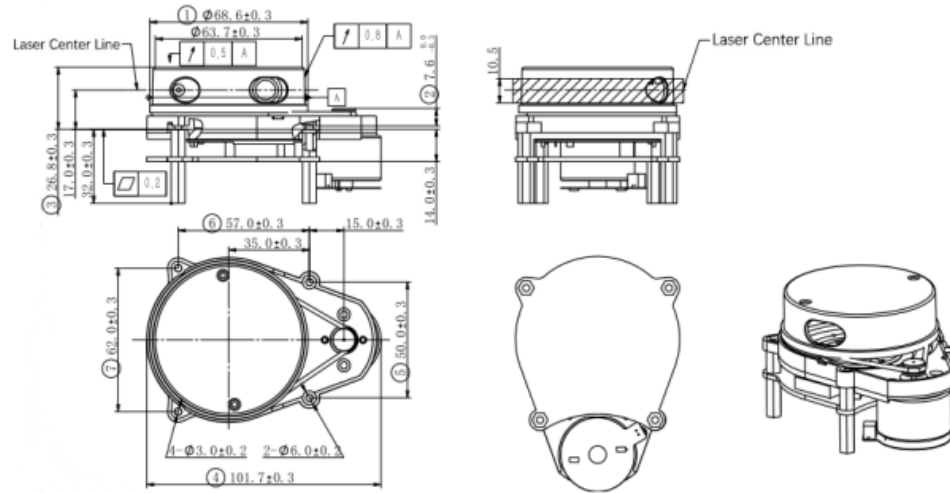
1.3 Installation and Dimensions

FIG 1 YDLIDAR X4 INSTALLATION AND MECHANICAL DIMENSIONS (UNIT:MM)

2 SPECIFICATIONS

2.1 Performance Parameter

CHART 1 YDLIDAR X4 PRODUCT PARAMETER

Item	Min	Typical	Max	Unit	Remarks
Ranging frequency	/	5000	/	Hz	Ranging 5000 times per second
Motor frequency	6	/	12	Hz	PWM or voltage speed regulation
Ranging distance	0.12	/	10	m	Indoor environment with 80% Reflectivity
Field of view	/	0-360	/	Deg	/
Systematic error	/	2	/	cm	Range≤1m
Relative error	/	3.5%	/	/	1m<Range ≤6m
Tilt angle	0.25	1	1.75	Deg	/
Angle resolution	0.43 (frequency@ 6Hz)	0.50 (frequency@ 7Hz)	0.86 (frequency@ 12Hz)	Deg	Different motor frequency

Note 1: The measurement range and relative accuracy above are the factory FQC standard value based on 80% reflectivity object.

Note 2: The relative error value indicates the accuracy of the Lidar measurement. Relative error (mean value) = (average measured distance-actual distance)/actual distance *100%, sample size: 100pcs.

Note 3: Lidar is a precision device. Please avoid using Lidar under high or low temperature or strong vibration situation, which might cause an exceeded relative error.
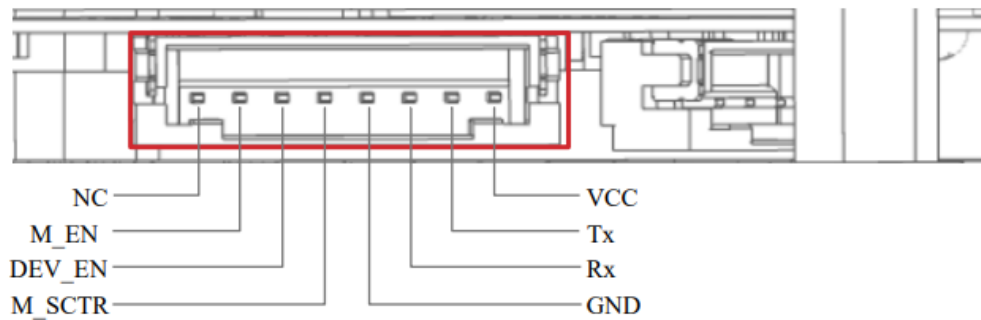
FIG 2 YDLIDAR X4 INTERFACES

CHART 3 YDLIDAR X4 INTERFACE DEFINITION

Pin	Type	Description	Defaults	Range	Remarks
VCC	Power supply	Positive	5V	4.8V-5.2V	/
Tx	Output	System serial port output	/	/	Data stream: LiDAR→Peripherals
Rx	Input	System serial port input	/	/	Data stream: Peripherals→LiDAR
GND	Power supply	Negative	0V	0V	/
M_EN	Input	Motor enables control terminal	3.3V	0V-3.3V	High level enables
DEV_EN	Input	Ranging enable control terminal	3.3V	0V-3.3V	High level enables
M_SCTR	Input	Motor speed control terminal	1.8V	0V-3.3V	Voltage speed regulation or PWM speed regulation
NC	/	Reserve pin	/	/	/

2.4 Data Communication

With a 3.3V level serial port (UART), users can connect the external system and the product through the physical interface. After that, users can obtain the real-time scanned point cloud data, device information as well as device status. The communication protocol of parameters are as follows:

AX-12A Servo Motor

AX-12+, AX-12A

1. Specifications

Item	Specifications
Baud Rate	7,843 [bps] ~ 1 [Mbps]
Weight	AX-12 (53.5 [g]), AX-12+ (53.5 [g]), AX-12A (54.6 [g])
Dimensions (W x H x D)	32 X 50 X 40 [mm] 1.26 X 1.97 X 1.57 [inch]
Resolution	0.29 [°]
Running Degree	0 ~ 300 [°] Endless Turn
Motor	Cored
Gear Ratio	254 : 1
Stall Torque	1.5 [N.m] (at 12 [V], 1.5 [A])
No Load Speed	59 [rev/min] (at 12V)
Operating Temperature	-5 ~ +70 [°C]
Input Voltage	9.0 ~ 12.0 [V] (Recommended : 11.1V)
Command Signal	Digital Packet
Physical Connection	TTL Level Multi Drop Bus Half Duplex Asynchronous Serial Communication (8bit, 1stop, No Parity)
ID	254 ID (0~253)
Feedback	Position, Temperature, Load, Input Voltage, etc
Gear Material	Engineering Plastic(Full)
Case Material	Engineering Plastic(Front, Middle, Back)

NOTE : Stall torque is the maximum instantaneous and static torque. Stable motions are possible with robots designed for loads with 1/5 or less of the stall torque.